HHS Public Access

Author manuscript

J Comput Assist Tomogr. Author manuscript; available in PMC 2017 July 01.

Published in final edited form as:

J Comput Assist Tomogr. 2016 ; 40(4): 589–595. doi:10.1097/RCT.0000000000000394.

Quantitative CT Classification of Lung Nodules: Initial Comparison of 2D and 3D Analysis

David S. Gierada, M.D.[*], **David G. Politte, Ph.D.**[*], **Jie Zheng, M.S.**[†], **Kenneth B. Schechtman, Ph.D.**[†], **Bruce R. Whiting, Ph.D.**[*,1], **Kirk E. Smith, B.S.**[*], **Traves Crabtree, M.D.**[‡], **Daniel Kreisel, M.D., Ph.D.**[‡], **Alexander S. Krupnick, M.D.**[‡], **G. Alexander Patterson, M.D.**[‡], **Varun Puri, M.D., M.S.C.I**[‡], and **Bryan F. Meyers, M.D., M.P.H.**[‡]

[*]Mallinckrodt Institute of Radiology, Washington University School of Medicine, Saint Louis, MO, 63110 Phone: 314-362-2927 Fax: 314-747-5970

[†]Department of Biostatistics, Washington University School of Medicine, Saint Louis, MO, 63110 Phone: 314-362-2927 Fax: 314-747-5970

[‡]Division of Cardiothoracic Surgery, Washington University School of Medicine, Saint Louis, MO, 63110 Phone: 314-362-2927 Fax: 314-747-5970

Abstract

Objective—To compare the performance of 2D and 3D quantitative CT methods for classifying lung nodules as lung cancer, metastases, or benign.

Materials and Methods—Using semiautomated software and computerized analysis, we analyzed more than 50 quantitative CT features of 96 solid nodules in 94 patients, in 2D from a single slice and in 3D from the entire nodule volume. Multivariable logistic regression was used to classify nodule types. Model performance was assessed by the area under the receiver-operating characteristic curve (AUC) using leave-one-out cross-validation.

Results—The AUC for distinguishing 53 primary lung cancers from 18 benign nodules and 25 metastases ranged from 0.79 to 0.83 and was not significantly different for 2D and 3D analyses (p=0.29–0.78). Models distinguishing metastases from benign nodules were statistically significant only by 3D analysis (AUC=0.84).

Conclusion—3D CT methods did not improve discrimination of lung cancer, but may help distinguish benign nodules from metastases.

Keywords

Lung nodule; CT; quantitative; 3D; computer-aided diagnosis

Corresponding author: David S. Gierada, M.D., Mallinckrodt Institute of Radiology, Box 8131, 510 South Kingshighway Boulevard, Saint Louis, MO 63110.

[1]Current affiliation: Department of Radiology, University of Pittsburgh School of Medicine, Pittsburgh, PA 15261

Conflicts of Interest: None

Introduction

Radiologists frequently encounter indeterminate lung nodules on CT examinations. Findings associated with an increased likelihood of malignancy, such as larger size, spiculated margins, and growth, support biopsy or resection. Nodules with less suspicious features, particularly smaller size, smooth rounded margins, and lack of growth typically are followed with serial CT examinations until features suspicious for malignancy develop (1, 2). Such surveillance of low risk lesions is intended to minimize the number of unnecessary invasive procedures for benign lesions, yet still allow diagnosis and treatment of the malignant lesions at an early stage.

Although CT surveillance may reduce the number of unnecessary invasive procedures, many still occur, with benign disease found in as many as 20% or more of pulmonary nodule resections (3–5). In addition, CT surveillance generates anxiety, effort, and increased medical costs even for benign lesions. For malignant nodules, CT surveillance delays biopsy, which could allow additional time for growth and metastasis. PET can be helpful in discriminating some benign and malignant lesions, but the metabolic activity in inflammatory and malignant nodules often overlaps, and PET is unreliable for nodules smaller than 1 cm diameter (6). Thus, despite an impressive array of technology, assessing the likelihood of malignancy quickly, accurately, and noninvasively remains a major challenge.

Previous investigators have developed reasonably successful prediction models to noninvasively discriminate benign from malignant nodules using combinations of clinical history and chest x-ray information (7–9). Other studies have found that computer-aided diagnosis using various quantitative features of pulmonary nodules on transverse CT sections can be moderately predictive of the benign or malignant nature of a nodule (10–12). However, a 2D transverse CT section samples only a small fraction of an entire pulmonary nodule, and 3D analysis of all spatial and attenuation information contained in the entire nodule might provide better classification. In this study, we hypothesized that three-dimensional (3D) volumetric CT quantitative analysis of lung nodules would improve the ability classify lung nodules compared to two-dimensional (2D) analysis. We also evaluated the additional impact of considering clinical information along with the CT data to enhance predictive ability.

Materials and Methods

Subject Eligibility

Patients ≥18 years of age scheduled for diagnostic and/or therapeutic resection of a pulmonary nodule ≤3 cm in greatest transverse dimension at our institution were identified from the daily clinic schedule of surgeons and enrolled by a study coordinator. Nodule size was confirmed by manual measurements on existing diagnostic CT images by one of the authors prior to enrollment (D.G.). The study was approved by the local institutional review board. Written informed consent was obtained from all subjects.

Clinical data collection

Subjects were interviewed using standardized forms to record history of hemoptysis, chronic obstructive pulmonary disease, emphysema, pulmonary fibrosis, other lung disease, and asbestos exposure. A detailed smoking history was obtained, including whether the patient had ever smoked; age began smoking; number of years smoked; amount smoked per day; and age of smoking cessation if applicable. Personal history and family history of cancer were elicited, including the cancer type and time since diagnosis.

CT imaging

All patients already had clinical chest CT scans performed prior to enrollment. For this study, an additional CT scan for quantitative nodule analysis was performed in each patient within one month prior to surgery. Scans were performed on a Definition 64 detector-row dual source scanner (Siemens), in single source mode, without intravenous contrast at full inspiration. To limit radiation exposure, the volumetric scan was targeted to the level of the nodule to be resected. In addition, thin-section images were obtained at 10 evenly spaced levels over the entire length of the lung to quantify emphysema (13).

The following technical parameters were used for both scanning protocols: 120 kVp; 130 mAs; automatic exposure control on; 0.33 second gantry rotation. For nodule scans, additional parameters included 0.6 mm detector collimation and pitch of 1.0. Nodule images were reconstructed at high spatial resolution, using a 102 mm field of view and 0.6 mm section thickness at 0.2 mm increments, to produce images with a voxel center spacing of 0.2 mm in each dimension. The B35f kernel was chosen for image reconstruction, after preliminary studies using a CTP657 phantom (The Phantom Laboratory) found that it provided the narrowest transition between materials of lung and soft tissue density among the available kernels that did not produce edge enhancement. Scans for quantifying emphysema were performed during a single, maximal inspiratory breath hold to acquire two contiguous 1 mm sections at each of the 10 evenly-spaced scan levels, at a field of view targeted to the widest diameter of the lungs.

Visual CT image analysis

The dedicated nodule CT scans were reviewed by a thoracic radiologist (D.G.), in conjunction with the preoperative clinical CT scans when necessary, to determine the lobe of each resected nodule and whether or not it was peripheral (within 2 cm of a pleural surface).

Quantitative CT image analysis

Nodule analysis—Nodules were segmented (separated) from the surrounding structures in the CT images with the software program 3D Slicer (version 4.0) (14) (Fig. 1). We used a 3D semiautomated iterative region growing method, starting from manually placed seed points, with region-growing according to whether the values of neighboring voxels were within a specified number of standard deviations of the region around the seeds; default values were used. Each segmented nodule was classified based on numerous quantitative CT parameters using software routines developed in MATLAB (Mathworks). Analyses of both 2D and 3D data were performed. For 2D analysis, only the single

transverse section containing the greatest cross-sectional area of the nodule was analyzed. The 3D analysis used the entirety of the segmented nodule volume. The quantitative CT parameters extracted included multiple variables related to nodule size, shape, attenuation, texture, and margin (see Supplemental Data for full details):

Size - Area and perimeter (2D); volume and surface area (3D).

Shape - Circularity (2D); Sphericity (3D); long: short axis ratio; primary (2D and 3D), secondary (2D and 3D), and tertiary (3D) moments of inertia.

Attenuation– Mean; median; standard deviation; variance; skewness; kurtosis; entropy.

Texture – These parameters were selected to quantify local and regional differences in attenuation that describe nodule homogeneity, contrast, and complexity. Parameters included mean, standard deviation, variance, skewness, kurtosis, and entropy of the difference image; lacunarity of the segmentation image at box sizes of 1, 2, 4, 8, 16, 32, 64, and 128 voxels (2D and 3D); and coarseness, contrast, busyness, complexity, and texture strength, each at distances of both 1 and 2 voxels.

Margin – These parameters were selected to quantify variations among nodules in surface contours. Parameters included the summed and mean distance to surface; normalized summed and mean distance to surface; fractal dimension of area or volume; fractal dimension of perimeter or surface; and gradient margin.

Emphysema analysis—Emphysema was quantified by the proportion of the lungs having attenuation lower than −950 HU, using the software program Emphysema Profiler (VIDA Diagnostics) (15).

Pathologic diagnosis

Surgical pathology was obtained from resection specimens. Resected nodules were classified from pathology reports as benign, primary lung cancer, or metastasis.

Data analysis

Comparisons were made between primary lung cancers and benign nodules, primary lung cancers and metastases, and benign nodules and metastases. These comparisons were made individually, to see how each of these nodule categories differed from each of the others by quantitative CT classification, and because distinction between two of these categories is often the primary clinical concern involving indeterminate lung nodules. Clinical and quantitative CT variables were compared using t-tests for continuous variables and chi-square tests for categorical variables. Continuous variables were tested for normality using the Kolmogorov-Smirinov test, and those with non-normal distribution were log transformed. Variables for which two-tailed P values were less than 0.10 in the univariable analysis were examined for use in multivariable modeling, with the aim of testing at least one variable from each quantitative CT category (size, shape, attenuation, texture, and margins) in the models if possible, without using an excessive number of variables relative

to the sample size. Fundamental parameters took precedence over those derived from the fundamental parameters (e.g., mean of the difference image took precedence over standard deviation of the difference image) if both had *p* values less than 0.10.

Multivariable models were created from clinical data alone, quantitative CT data alone, and combined clinical and quantitative CT data using stepwise logistic regression. A *P* value <0.05 was required for a variable to be retained in the model. Model performance was assessed by R^2 values and receiver operating characteristic curves using leave-one-out cross-validation. The areas under the receiver operating characteristic curves (AUC) were compared using the Mann-Whitney U test (16). Data were analyzed using SAS version 9.3.

RESULTS

Patients and Diagnoses

We enrolled 102 patients. Three patients did not undergo surgical resection after enrolling. Four patients were excluded due to technical inability of the segmentation program to separate the lung nodules from the chest wall. One patient was excluded due to pathologic and clinical uncertainty regarding whether the resected nodule was a primary lung cancer or a metastasis. Thus, 94 patients had complete data available for analysis. Two of these patients had two nodules in the same lung region that were scanned and resected, and each was treated as two independent samples. Thus, 96 nodules were analyzed.

The cohort consisted of 45 men and 49 women with a mean age of 62 yrs. ± 11 yrs. standard deviation (Table 1). Fifty-three of the nodules were primary lung cancer, 25 were metastases, and 18 were benign (Table 2). Eleven nodules were less than 1 cm in greatest transverse dimension, 44 were between 1 and 2 cm, and 41 were between 2 and 3 cm.

Primary Lung Cancer vs. Benign

Clinical Model—There were univariable differences at the *P*<0.10 level between groups (Table 1) for age, whether the patient had ever smoked, total years smoked, pack years smoked, and history of COPD. In stepwise logistic regression using these clinical parameters, the only significant parameter for distinguishing lung cancer from benign nodules was whether the patient had ever smoked (Model R^2=0.24; AUC=0.70) (Table 3).

2D CT Model—Of the 2D nodule parameters that differed at the *P*<0.10 level (Supplement Table S1), 10 were used in multivariable modeling: area, circularity, attenuation entropy, difference image mean, difference image entropy, lacunarity at box size=32 voxels, coarseness at distance=1 voxel, distance to surface normalized mean, fractal dimension of perimeter, and gradient margin. Area and circularity remained significant in the stepwise logistic regression model (Model R^2=0.30; AUC=0.79) (Table 3).

3D CT Model—Of the 3D nodule parameters that differed at the *P*<0.10 level (Supplement Table S2), those used in multivariable modeling were the same as or analogous to those used in 2D modeling: volume, sphericity, attenuation entropy, difference image mean, difference image entropy, lacunarity at box size=32 voxels, coarseness at distance=1 voxel, distance to surface normalized mean, fractal dimension of surface, and gradient

margin. Sphericity and difference image mean remained significant predictors of lung cancer in the stepwise logistic regression model (model R^2=0.32; AUC=0.80) (Table 3). The AUC of the 3D CT model was not statistically different from the AUC of the 2D CT model (p=0.78).

Combined Clinical-CT Models—In the combined model using parameters of the stepwise clinical and 2D CT models, whether the patient had ever smoked and nodule area were both significant predictors of lung cancer (model R^2=0.43; AUC=0.86) (Table 3). The AUC for the combined clinical-2D CT model was not statistically different from the AUC for the 2D CT model alone (P=0.24). In the combined model using parameters of the stepwise clinical and 3D CT models, whether the patient had ever smoked, sphericity, and difference image mean were all significant predictors (model R^2=0.47; AUC=0.88) (Table 3). The AUC of the combined clinical-3D CT model was not statistically different from the AUC of the 3D CT model alone (P=0.12). There was no significant difference between the AUC values of the combined clinical-2D CT model compared to the combined clinical-3D CT model (P=0.71).

Primary Lung Cancer vs. Metastasis

Clinical Model—There were univariable differences at the P<0.10 level (Table 1) for age, whether the patient had ever smoked, total years smoked, pack years smoked, history of COPD, and history of previous cancer. Because there were no patients with metastatic disease who did not have a history of previous cancer, we were unable to assess cancer history in the stepwise logistic regression model. Whether the patient had ever smoked and a history of COPD were significant variables in the stepwise model (R^2=0.31, AUC=0.77) (Table 4).

2D CT Model—Of the nodule parameters that differed between groups at the P<0.10 level (Supplement Table S3), 10 were used in logistic regression modeling: area, circularity, attenuation entropy, difference image mean, difference image entropy, lacunarity at box size=32 voxels, complexity at distance=2 voxels, distance to surface normalized mean, fractal dimension of perimeter, and gradient margin. Circularity and difference image entropy were significant in the final model (R^2=0.34, AUC=0.81) (Table 4).

3D CT Model—Of the 3D nodule parameters that differed at the P<0.10 level (Supplement Table S4), 10 of those used in multivariable modeling were the same as or analogous to those used in 2D modeling: volume, sphericity, attenuation entropy, difference image mean, difference image entropy, lacunarity at box size=32 voxels, complexity at distance=1 voxel, distance to surface normalized mean, fractal dimension of surface, and gradient margin. Coarseness at distance=1 voxel also was included. In the final model, only lacunarity at box size=32 voxels remained significant at P<0.05 (R^2=0.40, AUC=0.83) (Table 4). The AUC for the 3D CT model was not statistically different from the AUC of the 2D CT model (P=0.29).

Combined CT-Clinical Models—A history of COPD and circularity were significant in the combined clinical-2D CT model (model R^2=0.43; AUC=0.85). The AUC of the

combined clinical-2D CT model was not statistically different from the AUC of the 2D CT model alone (P=0.16). A history of COPD and lacunarity at box size=32 remained significant in the combined clinical-3D CT model (model R^2=0.56; AUC=0.90) (Table 4). The AUC of the combined clinical-3D CT model was significantly higher than the AUC of the 3D CT model alone (P=0.04). The AUC values of the combined clinical-2D CT and combined clinical-3D CT models were not significantly different (P=0.13).

Benign Nodule vs. Metastasis

Clinical Model—The only clinical parameter that differed at P<0.10 between those with benign nodules and those with metastases was a history of previous cancer. However, because there were no patients with metastatic disease who did not have a history of previous cancer, we were unable to assess cancer history by logistic regression modeling.

2D CT Model—Three of the nodule parameters that differed between groups at the P<0.10 level (Supplement Table S5) were used in 2D multivariable modeling: attenuation skewness, busyness at distance=2 voxels, and texture strength at distance=2 voxels. None of these parameters were significant at the P<0.05 level in stepwise logistic regression modeling; attenuation skewness was the strongest 2D parameter (p=0.062; model R^2=0.12; AUC=0.68).

3D CT Model—Nodule parameters that differed in 3D univariable comparisons at the P<0.10 level (Supplement Table S6) and were used in 3D multivariable modeling included attenuation skewness, standard deviation of difference image, skewness of difference image, lacunarity at box size=64, contrast at distance=2 voxels, busyness at distance=2 voxels, texture strength at distance=2 voxels, and complexity at distance=2 voxels. Skewness of the difference image (P=0.01) and lacunarity at box size=64 (P=0.03) remained significant predictors in the stepwise logistic regression model (model R^2=0.43; AUC=0.84).

Combined Clinical-CT Models—Due to the lack of testable clinical parameters, combined clinical-CT models for distinguishing benign nodules and metastases could not be created.

Discussion

In this initial study of a relatively small cohort, there was no difference in the ability of 2D and 3D analysis approaches to distinguish primary lung cancer from benign nodules or from metastases, and 3D analysis was superior to 2D analysis for distinguishing benign nodules and metastases. Thus, whether 3D nodule analysis is superior may depend on the types of nodules one wishes to discriminate, at least with the quantitative CT parameters tested. Whether 3D volumetry is superior to the current standard of 2D linear measurements for assessing change in size over time was not evaluated in this study.

Although it is disappointing and somewhat surprising that we did not find improvement in the ability to distinguish primary lung cancer from other nodule types with 3D analysis, 2D analysis may have some positive practical implications if equivalent to 3D. For example, quantitative 2D CT nodule classification could be applied to data sets that are not amenable

to 3D analysis, such as routine, non-thin section clinical scans on which indeterminate nodules are incidentally detected. It also could be applied in research using cases in existing publicly-available lung CT research databases that do not have many thin section CT cases needed for 3D analysis, such as those of the National Lung Screening Trial (17) and the Lung Imaging Database Consortium (18), without undue concern that diagnostic performance is being compromised. Reduced segmentation and nodule analysis time may be a minor practical benefit of the 2D approach. In addition, equivalence of 2D and 3D model performance would increase confidence that the predictive potential of non-contrast quantitative CT for lung nodule classification has been accurately estimated by 2D models developed previously.

Our quantitative CT models were moderately successful in discriminating nodule types, with AUC values ranging from 0.79–0.84. To illustrate the performance in other terms, in the 3D model distinguishing lung cancer from benign nodules (AUC=0.80), a probability cutoff for malignancy of 0.58 was associated with 87% sensitivity, 50% specificity, and correct predictions in 78% of cases. Other studies have found AUC values from 2D CT data prediction models of 0.83 to 0.92 (12, 19). A model that combined 2D and 3D nodule features achieved an AUC of 0.94 (20), while an entirely 3D classification system found an AUC of 0.83 for distinguishing 44 malignant from 52 benign nodules (21). In these comparison studies, pathologic proof was not obtained for most benign nodules and some presumed malignant nodules, whereas proof was obtained for all cases in our study. The nodules that were benign in our study may have been more challenging to classify than in other studies since they were of high enough concern to resect.

Analogous 2D and 3D input variables were used to create the multivariable models for distinguishing primary lung cancer from benign nodules and from metastases. However, the resultant 2D and 3D models did not contain only analogous variables, suggesting that the relative influence of these variables may differ depending on whether nodules are analyzed in 2D or 3D, or that some of the variables may have been correlated with each other. In building the models for distinguishing metastases from benign nodules, the univariable analyses did not provide analogous input variables for multivariable regression, and only the 3D model was statistically significant. Additional notable features are that all of the models contain parameters that describe nodule texture, which may be difficult to evaluate visually, and that the texture feature of lacunarity was a discriminator of metastases from both primary lung cancer and benign nodules.

Previous clinical models developed using demographic, smoking, and medical history information also included some subjectively assessed nodule features, and found AUC values in the range of 0.79–0.89 (7, 9, 22). The clinical model in our study for differentiating lung cancer and benign nodules had a lower AUC of 0.70, but did not include any nodule features. The AUC values of our combined clinical-CT models were greater than those for our clinical or CT models alone; most of the differences were not statistically significant, but given the consistently greater values for the combined models there may be a trend that our sample size was not large enough to confirm with statistical significance.

Because there were no patients with lung metastases who did not have a history of extrathoracic malignancy, the predictive value of a history of previous malignancy could not be evaluated in the multivariable clinical models. The expected frequency of patients who meet this condition is low, so a much larger sample would be needed to quantify the discriminatory power of a history of previous malignancy. Because of an expected strong association between a history of malignancy and a metastatic etiology of a lung nodule, the performance of the clinical and combined models for distinguishing metastases from primary lung cancer and benign nodules was probably underestimated.

There are several limitations of this study. The relatively high ratio of CT variables tested to nodules analyzed, and potential intercorrelation among some CT variables, could have led to the identification of some statistically significant variables by chance. This is a common problem in lung nodule classification efforts, and multiple approaches to reducing the number of variables have been proposed (23). For this reason, we limited the number of variables used in the multivariable modeling. This issue has limited bearing on the results of our study, as it was not designed to develop and validate definitive prediction models, but rather to compare the performance of 2D and 3D models generated in the same manner using analogous variables. While the proportion of nodule types in the sample might influence performance of the models, the effect of this on the comparison of 2D and 3D approaches likewise should be limited. The size of our cohort was relatively small, reflecting the volume and proportion of nodule types found in a single academic thoracic surgery department over two years, so the results should be verified in other populations.

We conclude that 3D quantitative nodule analysis may not improve the ability to distinguish primary lung cancer from benign nodules or metastases compared to 2D analysis, but may improve the discrimination of benign nodules from metastases. To improve model performance, exploring other strategies may be worthwhile, such as devising quantitative CT descriptors with more discriminatory power, using other statistical or machine learning methods for feature selection and modeling, or incorporating growth rate into a model. Whether a validated nodule classification model that provides a probability of malignancy would improve patient management decisions will need to be assessed in a clinical trial setting. However, development of a widely generalizable, robust model will likely require a database of nodules much larger than those that have been previously used. Since evaluation of virtually all lung nodules includes a CT examination, there is realistic potential for application in clinical practice. Opportunity and need for this may increase now that lung cancer screening for high-risk individuals is recommended by the United States Preventive Services Task Force (24).

Supplementary Material

Refer to Web version on PubMed Central for supplementary material.

Acknowledgments

Financial support was provided by the Barnes-Jewish Hospital Foundation. Eileen Jacobs, R.T., Jasmine Lewis, B.S.B.A., Joanne Musick, R.N., B.S.N., and Kathy Taylor performed patient enrollment and data collection. Mike Harrod, R.T. and Tim Street, R.T performed the research CT scans.

This study was approved by the institutional review board at Washington University.

Supported by the The Foundation for Barnes-Jewish Hospital and Washington University Institute of Clinical and Translational Sciences grant UL1TR000448 from the National Center for Advancing Translational Sciences (NCATS) of the National Institutes of Health (NIH). The content is solely the responsibility of the authors and does not necessarily represent the official view of the NIH.

References

1. MacMahon H, Austin JH, Gamsu G, et al. Guidelines for management of small pulmonary nodules detected on CT scans: a statement from the Fleischner Society. Radiology. 2005; 237(2):395–400. [PubMed: 16244247]
2. Naidich DP, Bankier AA, MacMahon H, et al. Recommendations for the management of subsolid pulmonary nodules detected at CT: a statement from the Fleischner Society. Radiology. 2013; 266(1):304–17. [PubMed: 23070270]
3. Grogan EL, Weinstein JJ, Deppen SA, et al. Thoracic operations for pulmonary nodules are frequently not futile in patients with benign disease. Journal of thoracic oncology: official publication of the International Association for the Study of Lung Cancer. 2011; 6(10):1720–5.
4. Kuo E, Bharat A, Bontumasi N, et al. Impact of video-assisted thoracoscopic surgery on benign resections for solitary pulmonary nodules. Ann Thorac Surg. 2012; 93(1):266–72. discussion 72–3. [PubMed: 22075217]
5. Davies B, Ghosh S, Hopkinson D, Vaughan R, Rocco G. Solitary pulmonary nodules: pathological outcome of 150 consecutively resected lesions. Interactive cardiovascular and thoracic surgery. 2005; 4(1):18–20. [PubMed: 17670346]
6. Maffione AM, Grassetto G, Rampin L, et al. Molecular imaging of pulmonary nodules. AJR Am J Roentgenol. 2014; 202(3):W217–23. [PubMed: 24555617]
7. Gould MK, Ananth L, Barnett PG. A clinical model to estimate the pretest probability of lung cancer in patients with solitary pulmonary nodules. Chest. 2007; 131(2):383–8. [PubMed: 17296637]
8. Schultz EM, Sanders GD, Trotter PR, et al. Validation of two models to estimate the probability of malignancy in patients with solitary pulmonary nodules. Thorax. 2008; 63(4):335–41. [PubMed: 17965070]
9. Swensen SJ, Silverstein MD, Ilstrup DM, Schleck CD, Edell ES. The probability of malignancy in solitary pulmonary nodules. Application to small radiologically indeterminate nodules. Arch Intern Med. 1997; 157(8):849–55. [PubMed: 9129544]
10. Iwano S, Nakamura T, Kamioka Y, Ikeda M, Ishigaki T. Computer-aided differentiation of malignant from benign solitary pulmonary nodules imaged by high-resolution CT. Comput Med Imaging Graph. 2008; 32(5):416–22. [PubMed: 18501556]
11. McNitt-Gray MF, Hart EM, Wyckoff N, Sayre JW, Goldin JG, Aberle DR. A pattern classification approach to characterizing solitary pulmonary nodules imaged on high resolution CT: preliminary results. Med Phys. 1999; 26(6):880–8. [PubMed: 10436888]
12. Shah SK, McNitt-Gray MF, Rogers SR, et al. Computer-aided diagnosis of the solitary pulmonary nodule. Acad Radiol. 2005; 12(5):570–5. [PubMed: 15866129]
13. Pilgram TK, Quirk JD, Bierhals AJ, et al. Accuracy of emphysema quantification performed with reduced numbers of CT sections. AJR Am J Roentgenol. 2010; 194(3):585–91. [PubMed: 20173132]
14. Fedorov A, Beichel R, Kalpathy-Cramer J, et al. 3D Slicer as an image computing platform for the Quantitative Imaging Network. Magn Reson Imaging. 2012; 30(9):1323–41. [PubMed: 22770690]
15. Guo J, Reinhardt JM, Kitaoka H, et al. Integrated system for CT-based assessment of parenchymal lung disease. IEEE International Symposium on Biomedical Imaging. 2002:871–4.
16. DeLong ER, DeLong DM, Clarke-Pearson DL. Comparing the areas under two or more correlated receiver operating characteristic curves: a nonparametric approach. Biometrics. 1988; 44(3):837–45. [PubMed: 3203132]
17. https://biometry.nci.nih.gov/cdas/studies/nlst/.
18. https://wiki.cancerimagingarchive.net/display/Public/LIDC-IDRI.

19. Aoyama M, Li Q, Katsuragawa S, Li F, Sone S, Doi K. Computerized scheme for determination of the likelihood measure of malignancy for pulmonary nodules on low-dose CT images. Med Phys. 2003; 30(3):387–94. [PubMed: 12674239]

20. Li F, Aoyama M, Shiraishi J, et al. Radiologists' performance for differentiating benign from malignant lung nodules on high-resolution CT using computer-estimated likelihood of malignancy. AJR Am J Roentgenol. 2004; 183(5):1209–15. [PubMed: 15505279]

21. Way TW, Hadjiiski LM, Sahiner B, et al. Computer-aided diagnosis of pulmonary nodules on CT scans: segmentation and classification using 3D active contours. Med Phys. 2006; 33(7):2323–37. [PubMed: 16898434]

22. Li Y, Chen KZ, Wang J. Development and validation of a clinical prediction model to estimate the probability of malignancy in solitary pulmonary nodules in Chinese people. Clin Lung Cancer. 2011; 12(5):313–9. [PubMed: 21889113]

23. Lee MC, Boroczky L, Sungur-Stasik K, et al. Computer-aided diagnosis of pulmonary nodules using a two-step approach for feature selection and classifier ensemble construction. Artificial intelligence in medicine. 2010; 50(1):43–53. [PubMed: 20570118]

24. Moyer VA. Screening for Lung Cancer: U.S. Preventive Services Task Force Recommendation Statement. Ann Intern Med. 2013

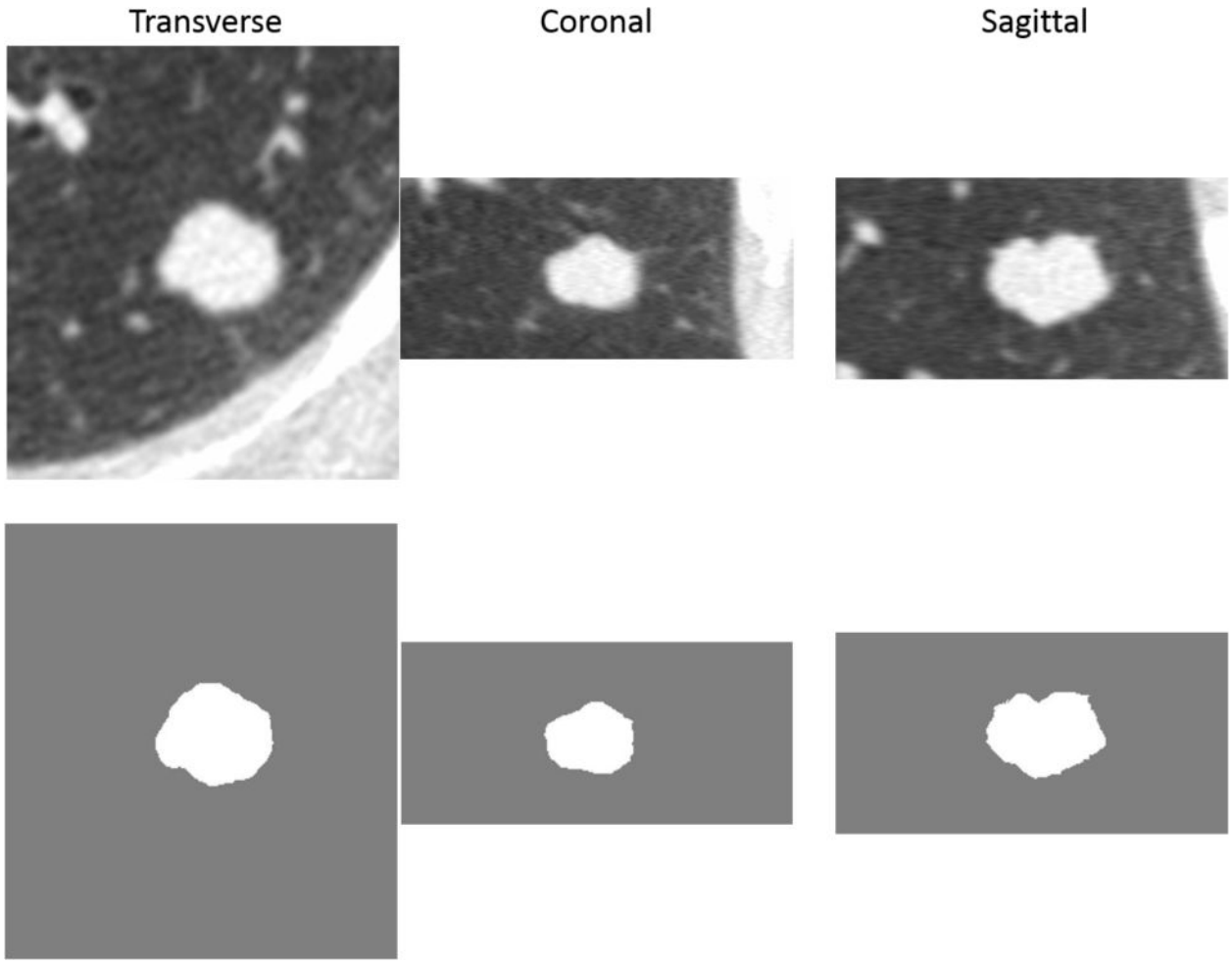

Figure 1.
Gray scale (top row) and binary segmented images of a 1.6 × 1.4 cm left lower lobe nodule. The diagnosis was adenocarcinoma.

Table 1

Comparisons of clinical parameters among patients with different nodule types.

			Lung Cancer(N=53)	Metastasis (N=25)	Benign (N=18)
Age, years[a,b]			65.0 +/− 10.1	60.1 +/− 11.1	57.7 +/− 10.9
Female, n(%)			31 (58.5%)	11 (44.0%)	8 (44.4%)
Caucasian, n(%)			48 (90.6%)	23 (92.0%)	17 (94.4%)
Ever smoked, n(%)[a,b]			48 (90.6%)	14 (56.0%)	9 (50.0%)
Among subjects ever smoked	**Total years smoked**[a]		36.4 +/− 14.0	26.9 +/− 15.0	26.9 +/− 15.0
	Pack years smoked		45.3 +/− 28.7	39.1 +/− 29.2	39.1 +/− 29.2
	Age started smoking, n(%)	**>19**	1 (11.1%)	1 (11.1%)	1 (11.1%)
		15–19	7 (77.8%)	7 (77.8%)	7 (77.8%)
		<15	1 (11.1%)	1 (11.1%)	1 (11.1%)
	Years quit smoking, n(%)	**>14**	4 (44.4%)	4 (44.4%)	4 (44.4%)
		1–14	2 (22.2%)	2 (22.2%)	2 (22.2%)
		<1	3 (33.3%)	3 (33.3%)	3 (33.3%)
Hemoptysis, n(%)			6 (11.3%)	0	2 (11.1%)
COPD, n(%)[a,b]			26 (49.1%)	2 (8.0%)	3 (16.7%)
Previous Cancer, n(%)[c]			14 (26.4%)	25 (100.0%)	6 (33.3%)
Family Cancer history, n(%)			40 (75.5%)	15 (60.0%)	12 (66.7%)
Nodule in upper/middle lobe, n(%)			37 (69.8%)	13 (52.0%)	11 (61.1%)
>2 cm from pleura, n(%)			7 (13.2%)	4 (16.0%)	1 (5.6%)
Pleural contact, n (%)			27 (50.9%)	12 (48.0%)	6 (33.3%)
Emphysema Index (%<−950 HU)			0.11 +/− 0.11	0.11 +/− 0.08	0.11 +/− 0.13
Upper Lung Index (%−950 HU)			0.12 +/− 0.13	0.10 +/− 0.10	0.11 +/− 0.15
Lower Lung Index (%−950 HU)			0.11 +/− 0.11	0.10 +/− 0.08	0.11 +/− 0.13

[a] $P<0.1$, lung cancer vs. benign

[b] $P<0.1$, lung cancer vs. metastasis

[c] $P<0.1$, metastasis vs. benign

Table 2

Nodule pathology.

Lung Cancer (N=53)	**Metastases (N=25)**	**Benign (N=18)**
Invasive adenocarcinoma (N=32)	Colon adenocarcinoma (N=5)	Granuloma (N=9)
Minimally invasive adenocarcinoma (N=6)	Head and neck squamous cell carcinoma (N=4)	Organizing pneumonia (N=4)
Squamous cell carcinoma (N=6)	1 each:	Hamartoma (N=3)
Carcinoid tumor (N=4)	Endometrial adenocarcinoma	Leiomyoma (N=1)
Small cell carcinoma (N=3)	Ethmoid spindle cell carcinoma	Dystrophic calcification (N=1)
Undifferentiated or unspecified (N=2)	Forearm nerve sheath sarcoma	
	Knee synovial cell sarcoma	
	Lower extremity fibrosarcoma	
	Lung squamous cell carcinoma	
	Ovarian adenocarcinoma	
	Pancreatic neuroendocrine carcinoma	
	Parotid melanoma	
	Penis leiomyosarcoma	
	Pleural fibrosarcoma	
	Thigh hemangiopericytoma	
	Thigh malignant fibrous histiocytoma	
	Thigh melanoma	
	Thyroid poorly differentiated carcinoma	
	Uterine leiomyosarcoma.	

J Comput Assist Tomogr. Author manuscript; available in PMC 2017 July 01.

Table 3

Multiple logistic regression models for distinguishing primary lung cancer from benign nodules.

Model	Variable	OR[a]	95% CI	*P* value	R^2	AUC[b]
Clinical	Ever smoked	9.6	2.6–35.4	0.001	0.24	0.70
2D CT	Area[c]	3.39	1.18–9.77	0.024	0.30	0.79
	Circularity (unit=0.01)	0.94	0.89–1.00	0.049		
3DCT	Difference image mean[c]	0.28	0.11–0.71	0.008	0.32	0.80
	Sphericity (unit=0.01)	0.91	0.85–0.98	0.010		
Clinical-2D CT combined	Ever smoked	14.0	2.9–68	0.001	0.43	0.86
	Area	6.1	1.8–20.6	0.021		
Clinical-3D CT combined	Ever smoked	11.5	2.2–59.9	0.004	0.47	0.88
	Difference image mean	0.22	0.07–0.69	0.01		
	Sphericity	0.91	0.85–0.99	0.021		

[a] Odds ratio (OR) >1 indicates higher likelihood of lung cancer as CT parameters increase one unit. Change unit for circularity and sphericity is 0.01.

[b] Area under receiver operating characteristic curve.

[c] Log transformed values

Table 4

Multiple logistic regression models for distinguishing primary lung cancer from metastases.

Model	Variable	OR[a]	95% CI	*P* value	R^2	AUC[b]
Clinical	COPD	7.09	1.43–35.2	0.017	0.31	0.77
	Ever smoked	4.03	1.13–14.4	0.031		
2D CT	Circularity (unit=0.01)	0.94	0.89–0.98	0.006	0.34	0.81
	Difference image entropy [c]	0.49	0.02–1.00	0.047		
3DCT	Lacunarity at box size=32 (unit=0.01)	4.1	1.8–9.3	0.001	0.40	0.83
Clinical-2D CT combined	COPD	10.1	2.04–50.2	0.001	0.43	0.85
	Circularity (unit=0.01)	0.92	0.88–0.97	0.005		
Clinical-3D CT combined	Lacunarity at box size=32 (unit=0.01)	1.10	1.04–1.16	0.001	0.56	0.90
	COPD	15.5	2.65–90.5	0.002		

[a] Odds Ratio (OR) >1 indicates higher likelihood of primary lung cancer as CT parameters increase one unit. Change unit for circularity and lacunarity is 0.01.

[b] Area under receiver operating characteristic curve

[c] Log transformed values